Applied Geochemistry 98 (2018) 127–140

Contents lists available at ScienceDirect

Applied Geochemistry

journal homepage: www.elsevier.com/locate/apgeochem

Regional patterns in the geochemistry of oil-field water, southern San Joaquin Valley, California, USA

Peter B. McMahon[a,*], Justin T. Kulongoski[b], Avner Vengosh[c], Isabelle M. Cozzarelli[d], Matthew K. Landon[b], Yousif K. Kharaka[e], Janice M. Gillespie[b], Tracy A. Davis[b]

[a] U.S. Geological Survey, Denver Federal Center, MS 415, Lakewood, CO, 80225, United States
[b] U.S. Geological Survey, 4165 Spruance Rd, San Diego, CA, 92101, United States
[c] Division of Earth and Ocean Sciences, Nicholas School of the Environment, Duke University, Durham, NC, 27708, United States
[d] U.S. Geological Survey, 12201 Sunrise Valley Dr., MS 430, Reston, VA, 20192, United States
[e] U.S. Geological Survey, 345 Middlefield Rd., Menlo Park, CA, 94025, United States

ARTICLE INFO

Editorial handling by Prof. M. Kersten.

Keywords:
Oil-field water
Geochemistry
Produced water
Injection

ABSTRACT

Chemical and isotopic data for water co-extracted with hydrocarbons in oil and gas fields are commonly used to examine the source of the formation water and possible impacts on groundwater in areas of oil and gas development. Understanding the geochemical variability of oil-field water could help to evaluate its origin and delineate possible contamination of shallow aquifers in cases where oil-field water is released to the environment. Here we report geochemical and multiple isotope (H, C, O, Sr, Ra) data from 22 oil wells, three sources of produced water that are disposed of in injection wells, and two surface disposal ponds in four oil fields in the southern San Joaquin Valley, California (Fruitvale, Lost Hills, North and South Belridge). Correlations between Cl and $\delta^{18}O$, as well as other ions, and gradual increases in salinity with depth, indicate dilution of one or more saline end-members by meteoric water. The saline end-members, represented by deep samples (610 m–2621 m) in three oil-bearing zones, are characterized by Na−Cl composition, near-seawater Cl concentrations (median 20,000 mg/L), enriched $\delta^{18}O$−H_2O (median 3.4‰), high ammonium (up to 460 mg-N/L), and relatively high radium activity ($^{226}Ra + ^{228}Ra$ = 12.3 Bq/L). The deepest sample has low Na/Cl (0.74), high Ca/Mg (5.0), and low $^{87}Sr/^{86}Sr$ (0.7063), whereas the shallower samples have higher Na/Cl (0.86–1.2), Ca/Mg near 1, and higher $^{87}Sr/^{86}Sr$ (~0.7083). The data are consistent with an original seawater source being modified by various depth and lithology dependent diagenetic processes. Dilution by meteoric water occurs naturally on the east side of the valley, and in association with water-injection activities on the west side. Meteoric-water flushing, particularly on the east side, results in lower solute concentrations (minimum total dissolved solids 2730 mg/L) and total radium (minimum 0.27 Bq/L) in oil-field water, and promotes biodegradation of dissolved organic carbon and hydrocarbon gases like propane. Acetate concentrations and $\delta^{13}C$ of dissolved inorganic carbon indicate biogenic methane production occurs in some shallow oil zones. Natural and human processes produce substantial variability in the geochemistry of oil-field water that should be considered when evaluating mixing between oil-field waters and groundwater. The variability could result in uncertainty as to detecting the potential source and impact of oil-field water on groundwater.

1. Introduction

Substantial recent research has examined the potential effects of oil and gas production activities on groundwater quality (Kharaka and Otton, 2007; Darrah et al., 2014; Humez et al., 2016; Schloemer et al., 2016; Wen et al., 2016; McMahon et al., 2017; Nicot et al., 2017; Zheng et al., 2017; Kulongoski et al., 2018). Quantifying mixing between groundwater and fluids from hydrocarbon reservoirs requires an understanding of the geochemical signatures of the end-member waters. Oil-field water consists of a complex mixture of inorganic and organic chemicals; therefore, measuring geochemical tracers with a range of chemical and physical properties could be advantageous to

* Corresponding author.
E-mail addresses: pmcmahon@usgs.gov (P.B. McMahon), kulongos@usgs.gov (J.T. Kulongoski), vengosh@duke.edu (A. Vengosh), icozzare@usgs.gov (I.M. Cozzarelli), landon@usgs.gov (M.K. Landon), ykharaka@usgs.gov (Y.K. Kharaka), jmgillespie@usgs.gov (J.M. Gillespie), tadavis@usgs.gov (T.A. Davis).

https://doi.org/10.1016/j.apgeochem.2018.09.015
Received 18 June 2018; Received in revised form 17 September 2018; Accepted 20 September 2018
Available online 21 September 2018

understanding mixing and contamination processes (Warner et al., 2014; Harkness et al., 2015; Lauer et al., 2016; Barry et al., 2018). For example, the combined use of noble gases, hydrocarbon-gas and trace-element abundances, dissolved salts isotopes, and water isotopes was shown to be a powerful approach for understanding natural and anthropogenic mixing processes involving shallow groundwater and fluids from natural-gas reservoirs in the northern Appalachian Basin (Darrah et al., 2014; Harkness et al., 2017).

Data sets for various chemical components in fluids from hydrocarbon reservoirs are available in the literature (Carothers and Kharaka, 1980; Land and Macpherson, 1992; Ballentine and Sherwood Lollar, 2002; Orem et al., 2014; McIntosh et al., 2010; Rowan et al., 2011; Blondes et al., 2017). However, the historical data sets can have limitations. Generally, they provide detailed information on a subset of constituents, depending on the research objectives, rather than data for a broad spectrum of constituents. Moreover, data may not be available for all the types of water associated with hydrocarbon production, such as native formation water, fluids used for enhanced oil recovery (EOR) and well stimulation treatment (WST), and oil-field wastewater-injection fluids (collectively referred to herein as oil-field water). Previous studies analyzed oil-field water in the southern San Joaquin Valley (SJV), California for various subsets of constituents, including the abundance and (or) isotopic composition of water, major and trace elements, organic acids, hydrocarbon gases, radium, and noble gases (Kharaka and Berry, 1973; Carothers and Kharaka, 1978; Schultz et al., 1989; Fisher and Boles, 1990; California Department of Conservation, 1996; Lillis et al., 2007; Tyne et al., 2018). We are not aware of any studies in the SJV that analyzed these chemical constituents in oil-field waters simultaneously. Such an analysis is essential for developing a comprehensive understanding of the sources and modification of oil-field water, and for applying that information to studies of mixing between groundwater and oil-field water. Oil fields in the SJV, like most oil fields, are characterized by variable geology and hydrocarbon production depths, but also by widely varying amounts of meteoric-water flushing and fluid injection for EOR, oil-field wastewater injection, and WST (Jordan and Heberger, 2014; California Department of Conservation, 2018a). Regional patterns in the geochemistry of oil-field water in the SJV are likely related to spatial variability in these oil-field characteristics.

This study examines oil-field water along an east-west transect in the SJV with the purpose of characterizing regional variability in the geochemistry of oil-field water and understanding the primary processes affecting it. The work was done in cooperation with the California State Water Resources Control Board in support of their Regional Groundwater Monitoring in Areas of Oil and Gas Production Program (California State Water Resources Control Board, 2018). From 2014 to 2017, water and gas samples were collected from 22 oil wells, three sources of produced water that are disposed of in injection wells, and two surface disposal ponds in four oil fields (Fig. 1). The sampled wells vary in terms of geology of the producing formation, depth of production, proximity to subsurface injection, and from never having been hydraulically fractured to having been hydraulically fractured within 2 weeks of sampling. To evaluate the possible sources and geochemical processes that affect both the inorganic and organic constituents in the oil-field water, samples were analyzed for a broad spectrum of inorganic and organic chemicals, isotopes, and gases. Data collected for this study were augmented with publicly available historical data. We posit that such a detailed characterization of the geochemical composition of oil-field waters is required in order to delineate the source of contamination in cases where oil-field water is released to the environment. Thus, this study provides a geochemical baseline for future studies that attempt to evaluate the possible impact of oil-field water on water resources in the SJV.

2. Geologic setting and oil field information

The Fruitvale, Lost Hills, and North and South Belridge oil fields, located in Kern County, at the southern end of the SJV (Fig. 1A), are the focus of this study. The SJV represents the southern part of the Central Valley of California, a 700-km-long asymmetric basin containing > 7500 m of Mesozoic through Cenozoic-aged sediments (Scheirer and Magoon, 2007). The Fruitvale oil field is on the east side of the SJV and the other fields are on the west side of the valley. Near Kern County, the SJV is bounded on the east by granitic rocks of the Sierra Nevada, on the west by marine sediments of the Temblor Range, part of the Coast Ranges, and on the south by the Tehachapi and San Emigdio Mountains. The following is a brief overview of the geologic setting in each field. Further details are in the Supplementary Information (SI) Section S1.

For this study, six samples from the Fruitvale oil field were collected from oil and gas wells producing from sands in the Santa Margarita (Miocene), Chanac (Miocene-Pliocene), and Etchegoin (Pliocene) Formations (Table S1 and Figs. S1 and S2) (Hluza, 1965; California Department of Conservation, 1998). The Chanac Formation consists of nonmarine sediments largely deposited in fluvial environments, whereas the Santa Margarita and Etchegoin sediments were largely deposited in marine environments (Preston, 1931; Hluza, 1965). Depths to the top of perforations in the sampled wells ranged from about 960 to 1350 m below land surface (Table S1). About 87 million m^3 of water were injected for EOR and produced-water disposal (WD) from 1960 to 2017 (Fig. S3). WD accounted for most of the volume (California Department of Conservation, 2018a). The Kern River flows through the southern end of the field and is a major source of groundwater recharge in the area.

In the Lost Hills oil field, nine samples were collected from oil and gas wells producing from diatomite zones in the Monterey (Miocene) and Etchegoin Formations, and from the Cahn zone of Land (1984) in the Monterey Formation (Table S1 and Fig. S1) (California Department of Conservation, 1998). The diatomite zones consist of relatively pure diatomite to diatomaceous shale and sands deposited in a marine environment. Production from the diatomite zones is commonly stimulated by hydraulic fracturing because of the rock's low permeability (Jordan and Heberger, 2014). Depths to the top of perforations in the sampled wells ranged from about 400 to 640 m in diatomite zones and 1390–1460 m in the Cahn zone (Table S1). Lost Hills was second to South Belridge in terms of total volume of water and steam injection (~436 million m^3 from 1960 to 2017) (Fig. S3). From 2014 to 2017, EOR accounted for the largest amount of injection (~87%), followed by WD (~13%) and WST such as hydraulic fracturing (~0.1%) (Fig. 2) (California Department of Conservation, 2018a).

In the Belridge oil fields, seven samples were collected from oil and gas wells producing from sands in the Temblor (64-Zone sandstone of Taylor and Soule (1993)) (Oligocene) and Tulare (Pleistocene) Formations, and diatomite zones in the Monterey Formation (Table S1 and Fig. S1) (California Department of Conservation, 1998). The Tulare Formation sands were largely deposited in fluviodeltaic environments, whereas the 64-Zone sands were deposited in a marine environment (Taylor and Soule, 1993). Depths to the top of perforations in the sampled wells ranged from about 140 m in the Tulare Formation, 210–610 m in the Monterey, and 2620 m in the Temblor (Table S1). South Belridge had the largest total volume of water and steam injection of the four fields (~1400 million m^3 from 1960 to 2017) (Fig. S3). The largest amounts of injection in South Belridge were for EOR (~56%), followed by WD (~44%) and WST (~0.2%) (Fig. 2) (California Department of Conservation, 2018a).

3. Methods

Three categories of end-member fluids were characterized geochemically: (1) water and gas from important hydrocarbon production zones (collected from 22 oil wells), (2) produced water intended for

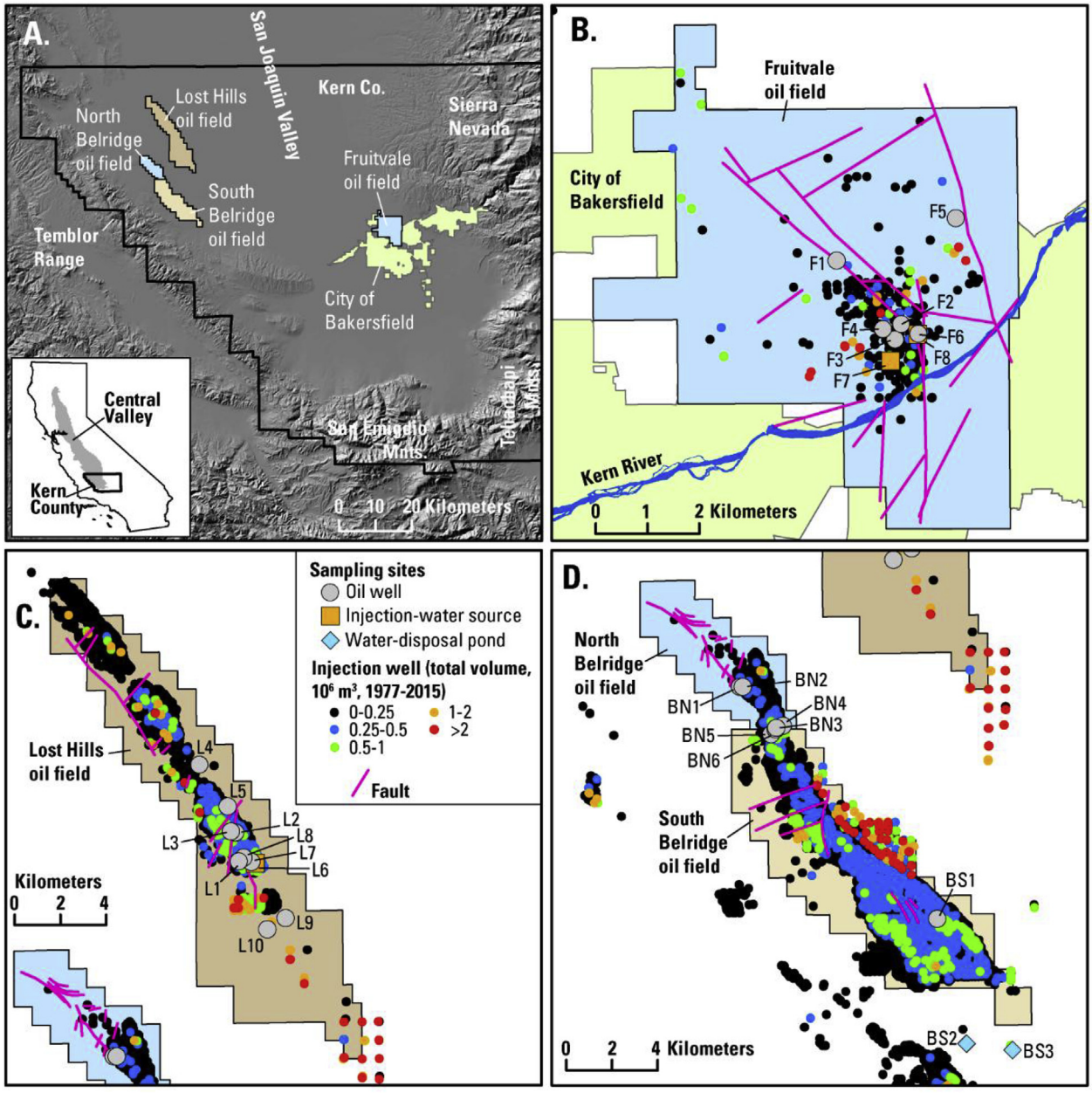

Fig. 1. Location of study-area oil fields and sampling sites. Injection-well volumes represent amounts of water or steam injected for enhanced oil recovery and wastewater injected for disposal, data from California Department of Conservation, 2018a).

disposal in injection wells (three sources), and (3) produced water disposed of in surface ponds (two ponds) (Fig. 1). The data are available in Tables S4 and S5, and in Gannon et al. (2018). The two sampled ponds receive water from multiple oil fields. The number and spatial distribution of samples in each category was limited somewhat due to difficulties gaining permission to access some sites. The selected sampling sites are intended to capture variability in the geology and depth of major production zones, history of EOR and hydraulic fracturing, and water types (relatively unimpacted formation water, formation water affected by mixing with fluids injected for EOR, treated produced water for injection, and discharge from recently hydraulically fractured wells).

3.1. Sample collection

Data collected for four general groups of analytes are discussed in this paper: (1) concentrations of dissolved inorganic and organic constituents, (2) concentrations of methane through pentane, (3) isotopes in selected components of groups 1 and 2, and (4) activities of ^{224}Ra, ^{226}Ra, and ^{228}Ra nuclides. Group 1 includes concentrations of major and minor ions and selected trace elements; dissolved organic carbon (DOC); and acetate. Group 3 includes δ^2H and δ^{18}O of water; δ^{13}C of dissolved inorganic carbon (DIC); ^{87}Sr/^{86}Sr of dissolved strontium; δ^{13}C of methane, ethane, and propane; and δ^2H of methane. General sampling protocols are described by Lico et al. (1982), Engle et al. (2016), and Harkness et al. (2017, 2018). Water samples were collected in 19-L plastic carboys at the well head of oil wells, flow manifolds for produced water intended for injection disposal, or directly from disposal ponds using a submersible pump, and then processed at a central location. Additional samples for the analysis of hydrocarbon gases were collected and processed at the well heads and flow manifolds. Some oil wells also had separate sampling ports for casing gas. Casing-gas samples for hydrocarbon gases were also collected at those sites. The data show that gas abundances and isotopic

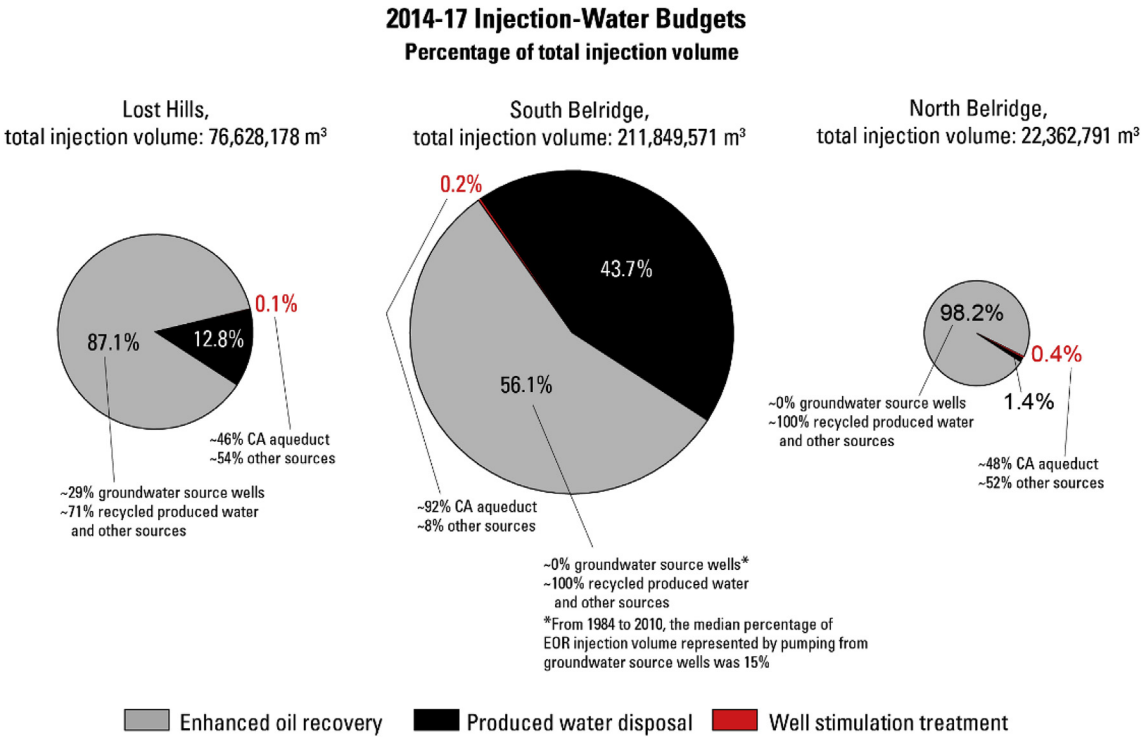

Fig. 2. Injection-water budgets for enhanced oil recovery, produced water disposal, and well-stimulation treatments in the Lost Hills, South Belridge, and North Belridge oil fields. Circle areas are proportional to total injection volumes. Data from California Department of Conservation (2018a).

compositions could vary depending on how the sample was collected (SI Section S2). Data from the wellhead samples are used in the analysis because they generally have $\delta^{13}C-CH_4$ and gas wetness values intermediate to those of the other sample types and because wellhead samples were the most common type of hydrocarbon-gas sample collected in this study. Various types of sample containers, filtering and preservation protocols were used, as listed in Table S2.

3.2. Sample analysis

Water and gas samples were analyzed by several U.S. Geological Survey (USGS) laboratories, Duke University, and private laboratories. The laboratories and their analytical procedures are listed in Table S3. The geochemical data discussed in this paper are listed in Table S4. These data and additional analytical data are also available from Gannon et al. (2018).

3.3. Quality control

Sampling equipment was cleaned or replaced after sampling each location. Nevertheless, blank and replicate samples represented about 40% of the samples collected for the study. Blank samples were collected by passing certified blank water obtained from the USGS National Water Quality Laboratory in Lakewood, Colorado through the cleaned or replaced sampling equipment using the same procedures as for environmental samples. Results for quality-control samples are listed in Table S5 and data are available from Gannon et al. (2018). Blank data indicate there were no issues with respect to sample contamination with target analytes during sample collection, shipping, or in the laboratory. Replicate data indicate reasonable reproducibility in the data, with > 90% of replicated constituents having relative standard deviations < 10%. Charge-balance errors were < 10% for all but two samples (10.3 and −12.7%) (Table S4). The sample (F5) with the 10.3% error was deficient in anions, which may reflect the fact that acetate was not analyzed in the sample. The sample (BN3) with the −12.7% error was deficient in cations, which may reflect the fact that K was not analyzed in the sample.

3.4. Historical data

Data collected for this study were augmented with historical data compiled from the State of California (California Department of Conservation, 2018a; Gans et al., 2018) and USGS (Blondes et al., 2017). For the most part, historical data consist of concentration data for major ions and trace elements. Samples that have absolute charge-balance errors < 10% are used in the analysis.

4. Results and discussion

4.1. Geochemical constraints on the origin of SJV oil-field waters

Increases in salinity (represented by Cl) and $\delta^{18}O-H_2O$ with depth, correlations between $\delta^{18}O-H_2O$ and Cl, and correlations between Na, Br, Li and Cl (Figs. 3 and 4), suggest the SJV oil-field waters represent one or more deep saline end-members, diluted by meteoric water. Samples BN5 (from arkosic sandstone, Temblor Formation, North Belridge), L9 (diatomaceous shale, Cahn zone, Monterey Formation, Lost Hills), and BN4 (diatomite zone, Monterey Formation, North Belridge) are relatively deep samples in their respective oil-bearing zones that are enriched in Cl and ^{18}O (Fig. 3, Table S1). Given that many of the chemical constituents such as Na, Br, and Li, as well as $\delta^{18}O-H_2O$, vary linearly towards the composition of one or more of those samples (Figs. 3 and 4), their compositions are used to characterize the chemistry of the saline end-members. In the following discussion, we evaluate the possible original saline source water, water-rock interactions that modified the composition of the saline source water to produce the observed chemistry of the saline end-members, and the nature of the mixing (dilution) process with meteoric water.

4.1.1. Original saline source water

The saline end-members (BN5, BN4, and L9) are characterized by Na–Cl compositions, near-seawater Cl concentrations (median

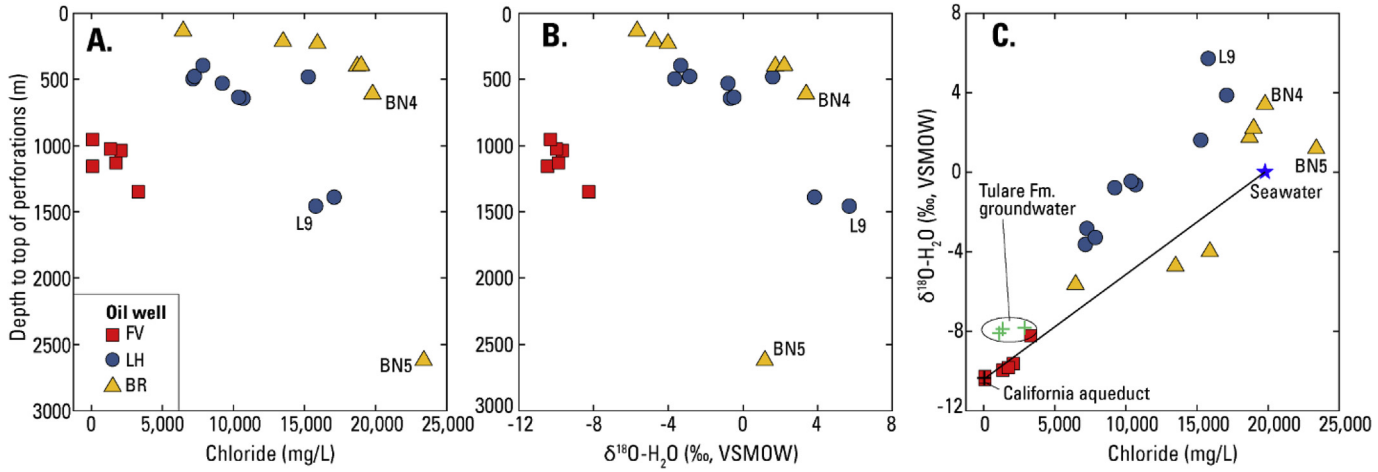

Fig. 3. A. Chloride and **B.** δ^{18}O-H_2O in oil-field water in relation to depth to the top of well perforations, **C.** δ^{18}O-H_2O in relation to chloride. FV, Fruitvale; LH, Lost Hills; BR, Belridge. California Aqueduct and Tulare groundwater data from Davis (2018).

20,000 mg/L), and enriched $\delta^{18}O-H_2O$ values (median 3.4‰). These data are generally consistent with previously reported data (Blondes et al., 2017) showing predominantly Na−Cl water compositions in the Belridge and Lost Hills fields and Cl concentrations up to ~27,000 mg/L (~760 mM) (Figs. S4 and 4). The deepest sample (BN5, ~2600 m) had low Na/Cl (0.74), high Br/Cl (~2×10^{-3}), and high Ca/Mg (5.0) molar ratios relative to modern seawater; and low $^{87}Sr/^{86}Sr$ (0.7063) (Fig. 4). Relative to BN5, the shallower samples (L9, ~1460 m; BN4, ~610 m) have higher Na/Cl (0.86–1.2), higher Br/Cl (~3×10^{-3}), lower Ca/Mg (near 1), and higher $^{87}Sr/^{86}Sr$ (~0.7083) ratios (Fig. 4). These geochemical variations are not consistent with the expected chemical composition of unaltered seawater or evaporated seawater, even though seawater is the most likely original formation water in these marine sediments (Fisher and Boles, 1990; Taylor and Soule, 1993). For example, the enriched $\delta^{18}O-H_2O$ (> seawater) is not consistent with the depleted $\delta^{2}H-H_2O$ (< seawater) (Fig. 5). The Br/Cl ratios could suggest evaporation of seawater (up to ~10-fold for BN5 and ~20-fold for L9 and BN4). However, 10-fold evaporation would not appreciably shift the seawater Na/Cl ratio toward the lower ratio in BN5. For L9 and BN4, 20-fold evaporation would lower Na/Cl ratios (~0.67), but that opposes the Na/Cl enrichment observed in those samples. Moreover, the highest historical Cl concentration in the Belridge fields (~27,000 mg/L) indicates < 1.5-fold evaporative concentration of seawater. The mismatches of $\delta^{18}O-\delta^{2}H$ and Br/Cl−Na/Cl indicate the saline end-members could not be unaltered residual seawater or evaporated seawater. The salinity also cannot be from salt dissolution given the Br/Cl ratios are inconsistent with halite dissolution that would generate Br/Cl < seawater. Also, there are no evaporite deposits in the section (Boles, 1998; Kharaka and Hanor, 2014). Consequently, we posit that the geochemical compositions of BN5, BN4, and L9 are derived from an original seawater source that was modified by depth (temperature) and lithology dependent water-rock interactions, consistent with interpretations of chemical data from other oil fields in the SJV (Schultz et al., 1989; Fisher and Boles, 1990; Boles, 1998).

4.1.2. Geochemical modifications induced by water-rock interactions

The data suggest multiple geochemical processes modified the original seawater source to produce the observed end-member water compositions. The end-member samples have $\delta^{18}O-H_2O$ and $\delta^{2}H-H_2O$ values that are greater than and less than seawater values (Fig. 5), respectively, with the deep end-member samples having the most enriched $\delta^{18}O-H_2O$ values in their respective oil-production zones (Fig. 3B). An increase in $\delta^{18}O-H_2O$ values with oil-well depth has been observed elsewhere in the SJV and attributed to temperature-dependent isotopic exchange between water and minerals (Kharaka and Berry, 1973; Fisher and Boles, 1990). This process appears to have occurred to some extent in all the fields (Fig. 3B). Relatively depleted $\delta^{2}H-H_2O$ values observed in our study area have also been observed in other SJV oil fields (Kharaka and Berry, 1973; Fisher and Boles, 1990). Fisher and Boles (1990) proposed that the ^{2}H depletion was due to isotopic equilibration between the water and detrital hydrous silicates or, possibly, between water and hydrocarbons.

Albitization of detrital plagioclase (i.e., replacement of calcic plagioclase by albite) is a common diagenetic process in sandstones (Boles, 1982) and has been reported in relatively deep and hot (100 °C–160 °C) sediments in central California (Schultz et al., 1989; Fisher and Boles, 1990; Taylor and Soule, 1993). Albitization appears to have affected the composition of the deepest end-member water (BN5) on the basis its low Na/Cl ratio (0.74) and Ca (and Sr) enrichment relative to seawater (Fig. 4). The combined Na depletion and Ca enrichment is consistent with the albitization process. Additionally, the low $^{87}Sr/^{86}Sr$ ratio in BN5 (0.7063) is not consistent with $^{87}Sr/^{86}Sr$ values for marine carbonates that mimic the isotope ratio of Oligocene seawater in which the BN5 sandstone was deposited (~0.7079–0.7083; Veizer, 1989) (Fig. 4H). We also exclude the possibility of dissolution of diagenetic carbonate cement in Oligocene sandstone from North Belridge as the source for Ca and Sr in BN5, given the carbonate's radiogenic $^{87}Sr/^{86}Sr$ ratios (average 0.7082; Taylor and Soule, 1993). Likewise, separated smectite minerals in sediments from the southern SJV were reported to have radiogenic ratios (0.708–0.714; Schultz et al., 1989). Instead, the low $^{87}Sr/^{86}Sr$ ratio in BN5 is more like those in separated plagioclase minerals from Oligocene and Miocene sandstones in the SJV (average 0.7066; Schultz et al., 1989). Based on the Sr isotopes variations, low Na/Cl, high Ca/Cl, and high Sr/Cl ratios, it is suggested that plagioclase alteration was the dominant source for the Ca and Sr in BN5.

While the deepest and most saline end-member (BN-5) is characterized by high Ca/Mg (~5), high Sr/Cl (~3×10^{-3}), and low $^{87}Sr/^{86}Sr$ (0.7063) ratios, the shallower end-members (BN4, L9) have lower Ca/Mg (~1) and Sr/Cl (~5×10^{-4}), and higher $^{87}Sr/^{86}Sr$ ratios (up to 0.7083) (Fig. 4). The higher $^{87}Sr/^{86}Sr$ ratios in BN4 and L9 suggest Sr was affected by water interactions with rocks characterized by higher $^{87}Sr/^{86}Sr$ compositions. We expect most lithology in the Monterey Formation to have higher $^{87}Sr/^{86}Sr$; including Miocene to Oligocene marine carbonates (0.7086–0.7089; DePaolo and Finger, 1991), diatomite and diatomaceous shale (0.7091–0.7115; Brueckner and Snyder, 1985; Weis and Wasserburg, 1987), and smectite minerals (0.708–0.714; Schultz et al., 1989). Ca/Mg ratios near 1 that characterize BN4 and L9 suggest water-rock interactions involving dolomite control Ca/Mg ratios in these shallower end-members.

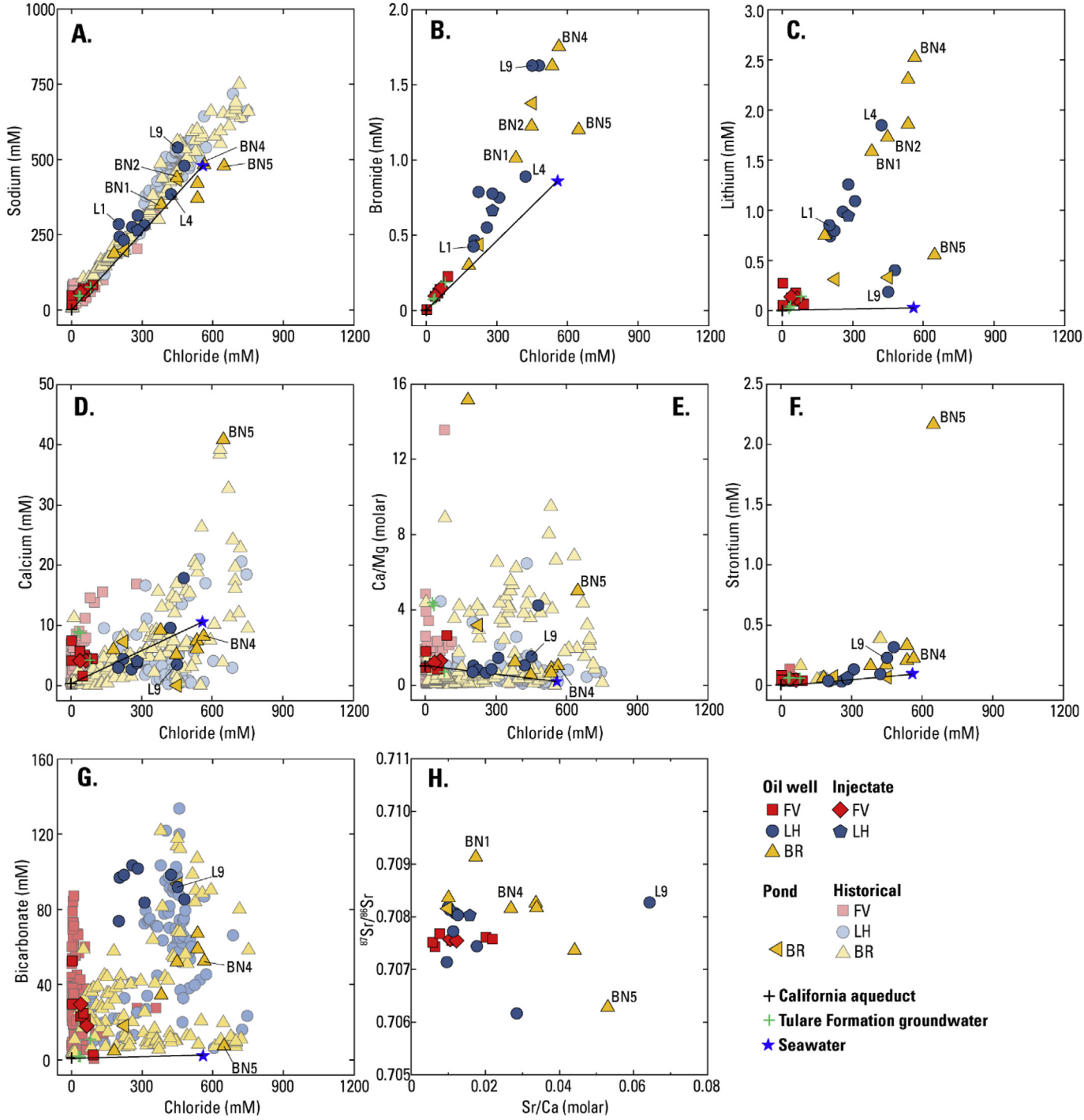

Fig. 4. (**A.–G.**) Concentrations and molar ratios of selected inorganic constituents in relation to chloride concentrations in oil-field water, (**H.**) $^{87}Sr/^{86}Sr$ in relation to strontium/calcium molar ratios. FV, Fruitvale; LH, Lost Hills; BR, Belridge. Aqueduct and Tulare groundwater data from Davis (2018); historical data from Blondes et al. (2017) and Gans et al. (2018).

All the end-member samples are enriched in Br relative to seawater (Fig. 4A). We have shown that the Br enrichment is not due to seawater evaporation, which means mineral or organic components in the formations are the likely Br source. Fisher and Boles (1990) attributed Br enrichment in water from some other SJV oil fields to organic sources based on a similarity in patterns of Br and I enrichment in their samples. This interpretation could explain the greater Br enrichment in end-members from the Monterey Formation (BN4, L9) than from the Temblor Formation (BN5), given the organic-rich nature of the Monterey Formation (Compton et al., 1992).

HCO_3 also occurs at much higher concentrations in BN4 and L9 (up to 5600 mg/L) than in the deeper BN5 (450 mg/L) or seawater (Fig. 4G). This suggests substantial amounts of HCO_3 are generated *in-situ* at shallower depths. This is discussed further in Section 4.2.1.

4.1.3. Effect of meteoric water and anthropogenic activities on the composition of oil-field waters

Most samples in the data set have $\delta^{18}O-H_2O$, Na, Br, Li, and Cl values that generally plot along mixing lines between relatively dilute meteoric water and one or more of the end-member waters (Figs. 3 and

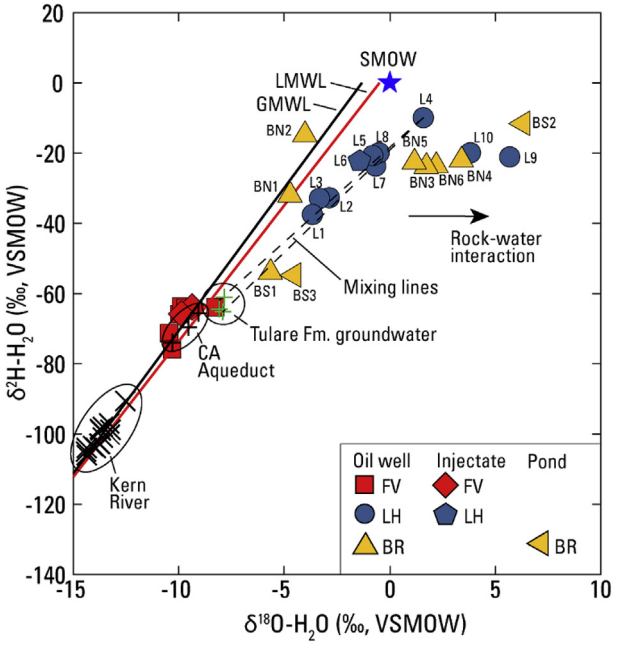

Fig. 5. Isotopic composition of oil-field water. FV, Fruitvale; LH, Lost Hills; BR, Belridge. SMOW, Standard Mean Ocean Water; GMWL, Global Mean Water Line (Rozanski et al., 1993); LMWL, Local Meteoric Water Line (Shelton et al., 2008); Kern River data from Coplen and Kendall (2000); California Aqueduct data from Williams and Rodoni (1997) and Davis (2018); Tulare groundwater data from Davis (2018).

4). Isotopic data show that oil-bearing zones in the Fruitvale field are more extensively flushed with meteoric water than oil-bearing zones in the Lost Hills and Belridge fields (Fig. 5). This flushing process contributes to oil-field water in Fruitvale having significantly ($p < 0.05$) lower concentrations of constituents such as B, Ba, Br, DOC, Li, Na, NH_4, Ra, and TDS compared to the Lost Hills and Belridge fields (Fig. S5). The Fruitvale samples came from wells with perforation depths of 956–1350 m, indicating relatively deep circulation of meteoric water in that area. Previous studies of oil fields on the east side of the SJV reported the presence of meteoric water in oil-producing formations to depths of ~1500 m (Fisher and Boles, 1990; Hayes and Boles, 1993). Fisher and Boles (1990) suggested deeply circulating meteoric water contributes to the extensive oil biodegradation observed on the east side. Unaltered meteoric water is less common in samples from the west-side oil fields even though many of the wells sampled on the west side are shallower than the Fruitvale wells (Fig. 3B).

The presence of deep meteoric water on the east side is probably due to substantial sources of recharge coming from Sierra Nevada streams, such as Kern River, sources that are absent on the west side. In addition, sandstones in the Fruitvale field are probably more permeable than diatomite on the west side (Schwartz, 1988; Coburn and Gillespie, 2002), and Fruitvale generally contains fewer major confining layers (Preston, 1931; Land, 1984), which could allow for deeper penetration of meteoric recharge on the east side. Fruitvale oil-field water is isotopically heavier than modern Kern River water (Fig. 5), suggesting the oil-field water was recharged under a different climatic or elevation regime than currently exists in the area. Davis and Coplen (1989) proposed that the isotopic composition of modern rivers draining the Sierra Nevada is lighter than the composition of rivers draining that area prior to about 400 ka ago when uplift of the Coast Ranges began, resulting in greater interception of moisture from the Pacific Ocean and more isotopically depleted precipitation in the Sierra Nevada. That interpretation suggests meteoric water in the Fruitvale oil-bearing zones was recharged during or prior to the middle Pleistocene.

Water from the Lost Hills and Belridge fields exhibits greater isotopic variability than water from Fruitvale, suggesting water in the fields on the west side of the valley have a more complex history than water on the east side. Diagenetic modifications associated with burial; natural mixing with meteoric water; mixing with injected fluids associated with EOR, WD, or WST; and evaporation of pond water could alter the isotopic composition of oil-field waters on the west side. The South Belridge and Lost Hills fields, for example, have had substantially more water injection than Fruitvale (Fig. S3). Most water injected in Lost Hills and Belridge during 2014-17 was recycled produced water, but about 30% of the water injected into the Lost Hills field for EOR during 2014-17 was groundwater withdrawn from the Tulare Formation adjacent to the field (Fig. 2), likely the major source of meteoric water introduced to the field. Groundwater was not a major source of water injected into the Belridge oil fields during that period, although it did account for about 15% of the water injected for EOR in South Belridge from 1984 to 2010 (Fig. 2). Water withdrawn from the California Aqueduct was a major source of water used in well stimulation treatment (WST), mostly hydraulic fracturing, but injections of water for WST were < 0.5% of total injections during 2014-17 and therefore represented a relatively small source of meteoric water injected into the oil fields (Fig. 2).

In Lost Hills, sample L4 is probably the least affected by fluid injection of all the samples from diatomite units, based on their proximities to injection wells and water-injection and WST histories (Fig. 1C, Table S1); therefore, L4 may be the most representative sample of unaltered formation water in the Lost Hills diatomite. The six remaining diatomite water samples (L1–L3, L5, L7, L8) generally plot along mixing lines between L4 and Tulare Formation groundwater (Fig. 5). The samples that appear to contain more meteoric water (L1–L3) had more injection within 100- and 500-m circular buffers around the wells, on average, than the three less mixed samples (L5, L7, L8) (Table S1), consistent with the proposed mixing scenario. The mixing trend is not considered to be related to hydraulic fracturing of these wells because at least 13 months had elapsed since the most recent WST in the sampled wells (Table S1). Injection of relatively fresh groundwater into oil-production zones can dilute chemical concentrations in those zone, which is observed in the Na, Cl, Br, Li, and TDS data for the Lost Hills diatomite samples (e.g. compare concentrations in L4 and L1 in Fig. 4 and Table S4).

Produced water recycled for EOR, or treated for WD, could also be a mixing endmember in Lost Hills and Belridge given its importance in the injection-water budget (Fig. 2). Whether mixing with recycled produced water can be resolved using water-isotope or other chemical data depends on how similar its composition is to the composition of formation water into which it is injected. The isotopic composition of the Lost Hills injectate sample (L6), for example, plots between that of presumed unaltered formation water (L4) and the samples with the largest meteoric-water fractions, but is like samples plotting between those two groups (Fig. 5). Thus, it is possible the samples with intermediate isotopic compositions only contained recycled produced water, which itself could contain a meteoric-water fraction. Recent analysis of noble gases in production gas and injectate streams from these same fields indicate noble gases could be a useful tracer for differentiating injected produced water from unaltered formation water (Barry et al., 2018; Tyne et al., 2018), regardless of other chemical similarities.

The three shallowest samples in the Belridge fields (BN1, BN2, BS1) also appear to contain some meteoric water. Although the two shallow wells in the diatomite zone (BN1, BN2) are located close to each other and have similar perforation depths (213–229 m), BN1 was hydraulically fractured two weeks before sampling using California Aqueduct water as the base fluid, whereas BN2 was hydraulically fractured about 2 years earlier (Table S1). The lighter isotopic composition in BN1 is consistent with a larger fraction of meteoric aqueduct water in that sample as a residual from the WST (Fig. 5). Recent injection of meteoric water into BN1 diluted concentrations of tracers like Na, Br, Li, and Cl compared to BN2 (Fig. 4). The dilution effects,

however, appear to be short-lived. The TDS concentration in BN1 was 24,600 mg/L at the time we sampled it, whereas a sample collected from BN1 by the operator one week after hydraulic fracturing had a TDS of 11,000 mg/L (California Department of Conservation, 2018b); and nearby well BN2 had a TDS concentration of 30,000 mg/L (Table S4). The data, indicating relatively rapid re-equilibration of TDS, suggest small-volume injections associated with WST can be a locally important, but transient, control on water chemistry.

The $^{87}Sr/^{86}Sr$ ratio in BN1 is noticeably more radiogenic than any other sample in our data set (Fig. 4H). It is not clear why this is so, but one potential source of ^{87}Sr is KCl (sylvite). For example, some Canadian sylvite deposits have $^{87}Sr/^{86}Sr$ ratios as high as 1.56 (Baadsgaard, 1987), which are much higher than the $^{87}Sr/^{86}Sr$ ratio in BN1. If KCl was present as an additive in the fluid used to stimulate BN1, this could account for the radiogenic $^{87}Sr/^{86}Sr$ signal in that well.

The shallowest oil-well sample in the data set, BS1 (top of perforations 136 m), has an isotopic composition like that of disposal-pond sample BS3 (Fig. 5). However, water sourced from a pond seems unlikely in this instance because BS3 is ~6 km from BS1 and the closest mapped disposal pond is ~1.5 km from BS1 (Central Valley Regional Water Quality Control Board, 2018). Alternative explanations for the isotopic composition of BS1 could include that it is affected by steam flooding for EOR or that it contains evaporated aqueduct or Tulare groundwater (Fig. 5). There were 121 steam-flood wells within 500 m of BS1, although not all were active at the time of sampling, whereas the other sampled wells in the Belridge fields had 0 to 2 steam-flood wells within 500 m (California Department of Conservation, 2018a). If the steam-flooding process fractionates water isotopes like geothermal systems, water in steam-flooded systems could become enriched in ^{18}O, with little effect on δ^2H, relative to meteoric water (Craig, 1966). An important unanswered question about that hypothesis is the lateral extent to which steam-flooding effects are transmitted in the flow system. In the South Belridge oil field, Tulare groundwater was withdrawn from wells near the east edge of the field as a source of injection water during 1984–2010 and was about 15% of the volume of injection for EOR during that period (California Department of Conservation, 2018a). This implies that Tulare groundwater could be a source of mixing in the South Belridge oil field. If so, sample BS1 may contain a mixture of this injected Tulare groundwater and native formation water.

4.2. Organic geochemical characterization of SJV oil-field waters

The organic geochemistry of oil-field water can play an important role in modifying the overall composition of the water (Carothers and Kharaka, 1980; Land and Macpherson, 1992; Kharaka and Hanor, 2014). Moreover, concentrations of organic components such as DOC, acetate, and hydrocarbon gases (C_1–C_5); and isotopic compositions of C_1–C_5 gases, in oil-field water can be substantially different from those in fresh groundwater, potentially making them useful tracers of mixing between groundwater and oil-field water (Thurman, 1985; Darrah et al., 2014; Kharaka and Hanor, 2014; Orem et al., 2014).

4.2.1. DOC and acetate

DOC and acetate concentrations in the samples of oil-field water range from about 6 to 2930 mg/L and < 1–911 mg/L, respectively (Fig. 6A and B). Maximum DOC concentrations in oil-field water from this study are comparable to those in produced water from some eastern shale plays, whereas the maximum acetate concentrations in SJV oil-field water are substantially higher than those in the shale plays (Orem et al., 2014). The observed acetate concentrations, however, are like those previously reported for SJV oil-field water (Carothers and Kharaka, 1978). DOC concentrations in the Fruitvale samples (median 32 mg/L) are significantly lower ($p < 0.05$) than concentrations in the samples from Lost Hills and Belridge (medians 155 mg/L and 170 mg/L, respectively) (Fig. S5J), and could reflect enhanced hydrocarbon biodegradation on the east side of the valley due to long-term meteoric water flushing (Fisher and Boles, 1990). Meteoric-water flushing could enhance the biodegradation of complex organic compounds in DOC and oil by delivering electron acceptors and nutrients, and lowering salinity and toxin levels (Milkov, 2011; Schlegel et al., 2013).

Even though the west-side fields have less meteoric-water flushing that Fruitvale, the decrease in acetate/DOC ratios with decreasing well-perforation depth in those fields is consistent with preferential biodegradation of labile organic compounds at shallow depths (Fig. 6E). Carothers and Kharaka (1978, 1980) proposed that lower formation temperatures (< 80 °C) in shallow oil-producing zones allow extensive biodegradation of acetate to occur. Thus, for labile organic compounds like acetate, formation temperature may be as important as meteoric-water flushing in the context of biodegradation. The low acetate/DOC ratios at shallow depths are also associated with heavy $\delta^{13}C$-DIC values (14.2‰–23.6‰) compared to deeper, acetate-enriched samples (−3.83 to 0.16‰) (Fig. 6F). Although acetate data are unavailable for Fruitvale, the deepest sampled well in that field (F6) also has the lightest $\delta^{13}C$-DIC value (6.49‰), consistent with the data from the west-side fields. Several studies proposed that heavy $\delta^{13}C$-DIC values in shallow oil reservoirs are due to biodegradation of oil under methanogenic conditions (Carothers and Kharaka, 1980; Jones et al., 2008; Milkov, 2011). Isotopic modeling of field and laboratory data by Jones et al. (2008) suggested methanogenic activity associated with oil biodegradation occurs primarily via the CO_2 reduction pathway, where secondary CO_2 from hydrocarbon biodegradation is the substrate, and secondarily by acetate fermentation. Cathles et al. (1987) proposed that CO_2 generation from isotopically heavy carbonate minerals during steam flooding accounted for the isotopically heavy CO_2 in the Buena Vista oil field, located south of the Belridge fields. Steam flooding probably cannot account for the heavy $\delta^{13}C$-DIC values in our samples because there were no steam-flood wells within 500 m of the sampled wells in Fruitvale and Lost Hills, and only 0–2 steam-flood wells within 500 m of the sampled wells in Belridge that had $\delta^{13}C$-DIC data (California Department of Conservation, 2018a).

Most samples from the three oil fields have much higher HCO_3 concentrations (up to ~7300 mg/L, 120 mM) than can be accounted for by mixing seawater with shallow meteoric water sources (Fig. 4G), indicating substantial *in-situ* HCO_3 production occurs. The high HCO_3 concentrations at shallower depths are associated with low acetate/DOC ratios and high $\delta^{13}C$-DIC values (Fig. 6), consistent with HCO_3 production associated with oil biodegradation and methanogenesis (Carothers and Kharaka, 1980; Jones et al., 2008; Milkov, 2011). At greater depths, samples BN5, L9, and L10 have variable HCO_3 concentrations, high acetate/DOC ratios, and low $\delta^{13}C$-DIC values (−3.8 to 0.2‰) (Fig. 6), indicating methanogenesis was less important. The $\delta^{13}C$ values of the deep samples are like the values for some marine carbonates (Keith and Weber, 1964), but dissolution of carbonate minerals in the absence of CO_2 production seems unlikely because the samples are supersaturated with respect to calcite and dolomite based on preliminary PHREEQC calculations (in situ water temperatures are not well constrained). Carothers and Kharaka (1980) proposed that HCO_3 with similarly low $\delta^{13}C$ values in deep zones in other SJV oil fields is produced by thermal degradation of organic matter. We also cannot rule out the possibility that SO_4 reduction produced CO_2 in the deeper samples given the relatively high detection levels for SO_4 in those samples (Table S4). Reaction of isotopically light CO_2 from SO_4 reduction with isotopically enriched dolomite cement (up to ~18‰ in SJV Miocene sediments; Murata et al., 1969), could produce the observed $\delta^{13}C$-DIC values in the deep samples.

4.2.2. Hydrocarbon gases

Oil-field water samples have δ^2H–CH_4 and $\delta^{13}C$–CH_4 values ranging from −246.0 to −187.7‰ and −46.65 to −38.96‰, respectively (Fig. 7A). Isotopic values in those ranges are generally indicative of thermogenic CH_4 (Schoell, 1980; Whiticar et al., 1986), and the

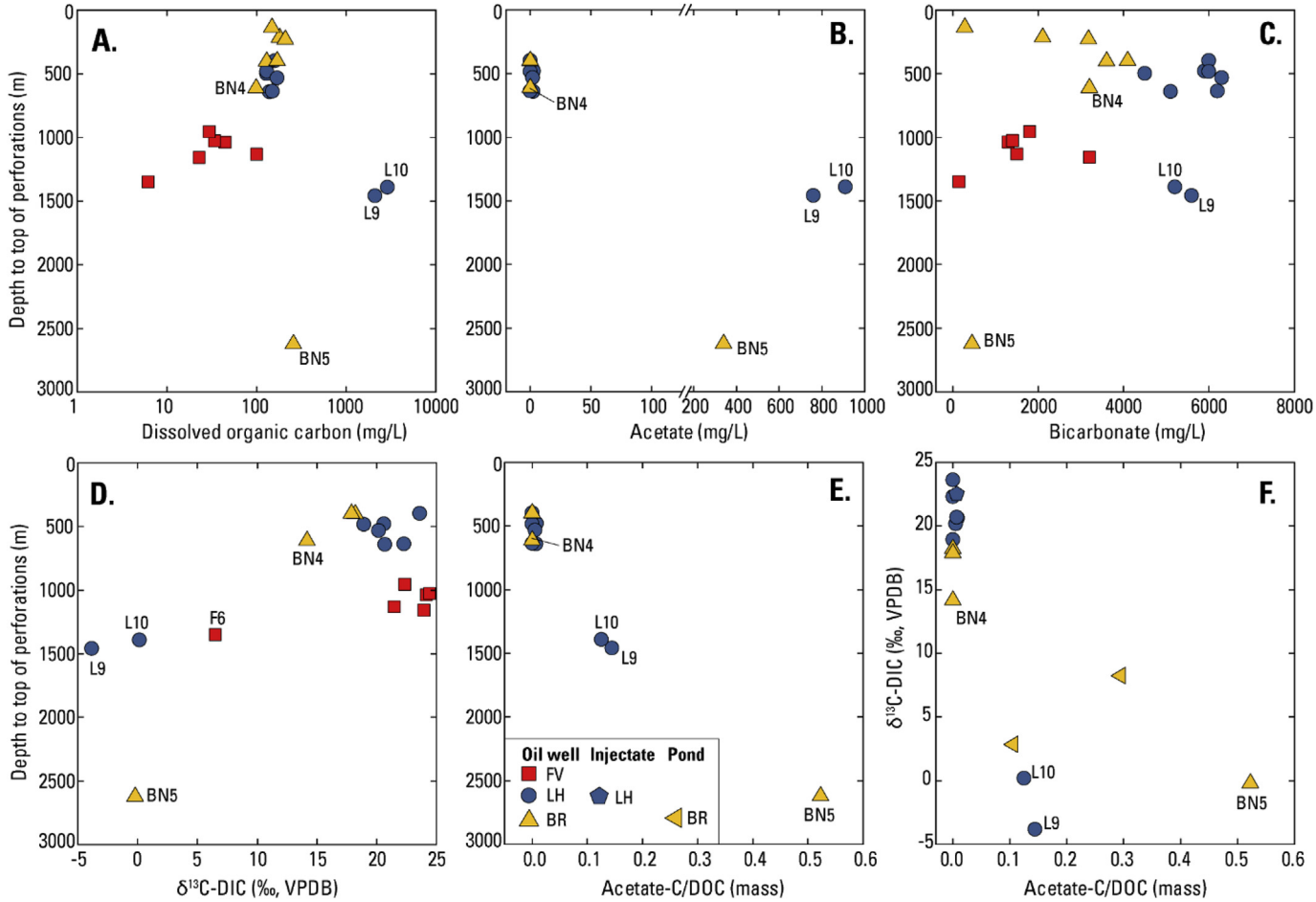

Fig. 6. Concentrations of (**A.**) DOC, (**B.**) acetate, and (**C.**) bicarbonate; and (**D.**) δ^{13}C-DIC, in oil-field water in relation to depth to the top of well perforations; (**E.**) depth to the top of well perforations and (**F.**) δ^{13}C-DIC in relation to acetate-C/DOC ratios in oil-field water. FV, Fruitvale; LH, Lost Hills; BR, Belridge. Acetate samples from Fruitvale were damaged during shipment to the laboratory.

presence of C_3–C_5 hydrocarbons in most of the samples supports that interpretation (Table S4). Interestingly, the acetate and δ^{13}C-DIC data suggest biogenic CH_4 production occurs in the shallower oil wells (Fig. 6D), yet the CH_4 isotopic data do not clearly indicate the presence of a biogenic CH_4 component based on the isotopic criteria established by Schoell (1980) and Whiticar et al. (1986) (Fig. 7A). This could indicate the fraction of biogenic CH_4 is small compared to the thermogenic-gas fraction. Additionally, Jones et al. (2008) showed that $\delta^{13}C$–CH_4 values in mixtures of biogenic and thermogenic gas could remain relatively heavy if a substantial fraction of the secondary CO_2 produced during oil biodegradation is converted to methane.

δ^{13}C data for CH_4, C_2H_6 (ethane), and C_3H_8 (propane) indicate the hydrocarbon gases themselves are also degraded to various extents. In Fruitvale and Lost Hills, $\delta^{13}C$–C_3H_8 values are as heavy as −6.3‰ and −10.4‰, respectively (Fig. 8). When compared to ranges of δ^{13}C values in 81 gas samples from the SJV reported by Lillis et al. (2007), C_3H_8 appears to be the most heavily degraded hydrocarbon, with lesser degradation of C_2H_6 and no apparent degradation of CH_4. Preferential degradation of C_3H_8 over CH_4 and C_2H_6 has been noted in numerous oil and gas fields (James and Burns, 1984; Milkov, 2011). The Fruitvale gases appear to contain the most heavily degraded C_3H_8 based on the δ^{13}C data, followed by the Lost Hills gases, a pattern that appears to generally correspond with the extent of meteoric-water flushing indicated by the δ^2H–H_2O and $\delta^{18}O$–H_2O data (Fig. 5). Sample L4, from Lost Hills, was an exception to the pattern. L4 contains some biodegraded C_3H_8 even though it does not contain substantial meteoric water.

Gas wetness values for the oil-field waters range from < 1 to ~50% (Fig. 7B). Wetness values in the Fruitvale field exhibit a narrow range near the threshold between wet and dry gas (2.5%) proposed by Lillis et al. (2007) for SJV gas, whereas values in the Lost Hills and Belridge fields exhibit much broader ranges in values. The combination of biogenic CH_4 production and preferential degradation of C_3H_8 in shallow oil-bearing zones could result in residual gas becoming drier (James and Burns, 1984; Milkov, 2011), and may explain the consistently low wetness values for the Fruitvale samples and some samples from the west-side fields (Fig. 7B). That combination of processes did not result in relative dry gas in all instances. Sample L2, from Lost Hills, has heavy δ^{13}C-DIC (20.6‰) and $\delta^{13}C$–C_3H_8 (−14.7‰) values (Table S4), indicating biogenic CH_4 production and C_3H_8 degradation occurred, but it still has the second highest wetness value (47%) (Fig. 7B). The wide range in gas wetness values in the Lost Hills and Belridge samples appear to reflect several factors, including the extent of microbial activity and probably initial gas wetness.

4.3. Other chemicals of concern in SJV oil-field waters

In addition to evaluating the source of the oil-field water and mechanisms of geochemical modification, here we report the occurrence of some other chemicals that are known to be enriched in oil-field waters, including ammonium and naturally occurring radioactive materials (NORM) in the form of radium nuclides. These chemicals could be of concern if oil-field water mixes with groundwater in the study area.

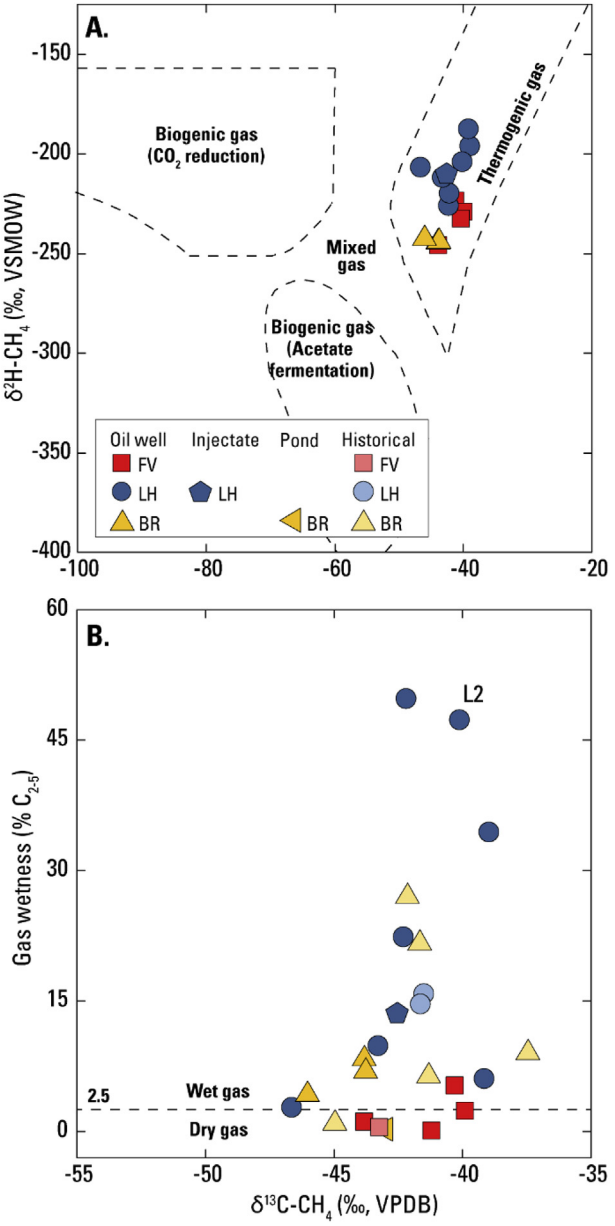

Fig. 7. (**A.**) δ^2H-CH_4 and (**B.**) gas wetness in relation to δ^{13}C-CH_4. FV, Fruitvale; LH, Lost Hills; BR, Belridge. In **A.**, methane source boundaries from Whiticar et al. (1986) and Schoell (1980). In **B.**, historical data and threshold value separating wet and dry gas from Lillis et al. (2007).

4.3.1. Ammonium

Previous work showed that water in hydrocarbon reservoirs could be enriched in NH_4 due to mineralization of organic N in the organic-rich sediments (Williams et al., 1995; Harkness et al., 2015). The Monterey Formation in the study area is also noted for NH_4-enriched sediment (Compton et al., 1992). Data from this study are consistent with that previous work. NH_4 concentrations range from 1.4 to 460 mg-N/L (Fig. 9), and are significantly lower ($p < 0.05$) in the Fruitvale field (median 5.8 mg-N/L) than in the Lost Hills and Belridge fields (medians 163 mg-N/L and 426 mg-N/L, respectively) (Fig. S5E). The large difference in NH_4 between Fruitvale and the west-side fields is consistent with meteoric-water flushing on geological timescales in Fruitvale, which could promote substantial biodegradation of organic carbon and removal or dilution of soluble degradation products from the system (Milkov, 2011; Schlegel et al., 2013). In the Lost Hills and Belridge fields, the patterns in NH_4 concentrations reflect variability in lithology of the oil-production zones and dilution effects due to EOR injection. In both fields, NH_4 concentrations are higher in the diatomite wells than in wells producing from other lithologies, consistent with the organic C-rich nature of the diatomite (Compton et al., 1992). Among the Lost Hills diatomite wells, the highest Cl and NH_4 concentrations occur in the well least affected by injection (L4; Fig. 5), and lower concentrations occur in the wells affected by injection of relatively dilute groundwater (Fig. 9), consistent with the effects of dilution.

4.3.2. Radium

Activities of ^{224}Ra, ^{226}Ra, and ^{228}Ra in filtered samples of oil-field water range from 0.09 to 4.8 Bq/L, 0.04–8.6 Bq/L, and 0.05–3.7 Bq/L, respectively (Table S4). Total radium (Ra_{total} = ^{224}Ra + ^{226}Ra + ^{228}Ra) activities range from 0.27 to 17 Bq/L. ^{224}Ra and ^{226}Ra account for significantly larger ($p < 0.05$) fractions of Ra_{total} (median 40% and 35%, respectively) than does ^{228}Ra (median 23%) (Fig. S6A). Measurements of ^{224}Ra in oil-field water are rare but the data suggest ^{224}Ra could be an important component of the Ra_{total} inventory in oil-field waters. Overall, the SJV oil-field waters have much lower Ra activities compared to oil-field brines from other basins in the U.S. The median ^{226}Ra + ^{228}Ra activity measured in this study (0.78 Bq/L) is much lower than median activities in produced water from the Marcellus and Bakken shales and Gulf Coast (91 Bq/L, 43 Bq/L, and 23 Bq/L, respectively) (Rowan et al., 2011; Lauer et al., 2016; Kraemer and Reid, 1984).

Radium activities in water depend, in part, on the salinity, pH, and redox state of the water (Kraemer and Reid, 1984; Vinson et al., 2013). Ra_{total} activities in samples from oil wells in Fruitvale (median 1.1 Bq/L) are significantly lower ($p < 0.05$) than activities in oil-well samples from Lost Hills and Belridge (medians 1.3 Bq/L and 3.5 Bq/L, respectively) (Fig. 10A and Fig. S5K). Our data show that the deepest and most saline water (BN5) has the highest Ra activity (17.1 Bq/L), consistent with the high-temperature model of formation of that water (see section 4.1) (Fig. 10). The other oil-field waters have lower Ra activities that are associated with the salinity variations (Fig. 10A; Cl−Ra Spearman correlation $r = 0.60$, $p = 0.003$). Previous studies showed that Ra activity in oil-field water generally increases with salinity due to other ions in saline water competing with Ra for adsorption sites on solids (Kraemer and Reid, 1984; Rowan et al., 2011). Ra_{total} activities are also positively correlated with concentrations of dissolved Fe(II) ($r = 0.45$, $p = 0.034$) (Fig. S6B). Positive correlations between Ra activities and Mn and Fe concentrations have been attributed to mobilization of Ra adsorbed onto Mn(IV)- and Fe(III)-oxide grain coatings following the reductive dissolution of those coatings (Szabo et al., 2012). Given the high Fe concentrations in some samples, it is also possible some Fe(II) was mobilized from the metal oil-well casings. Sample BN5 has a very low Fe(II) concentration (54 µg/L) but has the highest Ra_{total} activity in the data set (Fig. 10A and Fig. S6B). That sample was excluded from the Ra−Fe correlation analysis because it also has the highest Cl concentration in the data set (23,000 mg/L), suggesting Ra in the sample is related more to its high salinity than to its Fe concentration. Moreover, the 64-Zone sandstone from which that well produced is relatively clean sandstone that may contain less clay than the shallower diatomaceous shales (Fig. S1) (Taylor and Soule, 1993). A lack of clay in the sandstone could result in reduced capacity for Ra adsorption in that production zone, and higher dissolved Ra_{total} activities, regardless of the salinity (Vengosh et al., 2009).

^{228}Ra/^{226}Ra activity ratios range from 0.14 to 2.3 and are generally higher in the Fruitvale water samples (median 1.5) than in water from diatomite zones in the Lost Hills and Belridge fields (median 0.55) and Cahn zone in Lost Hills (median 0.24) (Fig. 10C). ^{226}Ra is part of the ^{238}U decay series and ^{224}Ra and ^{228}Ra are part of the ^{232}Th decay series. Subsurface waters are generally thought to have ^{228}Ra/^{226}Ra ratios like the Th/U activity ratios in rocks with which they come in contact, assuming secular equilibrium between ^{228}Ra and ^{232}Th and between ^{226}Ra and ^{238}U (Kraemer and Reid, 1984; Vengosh et al.,

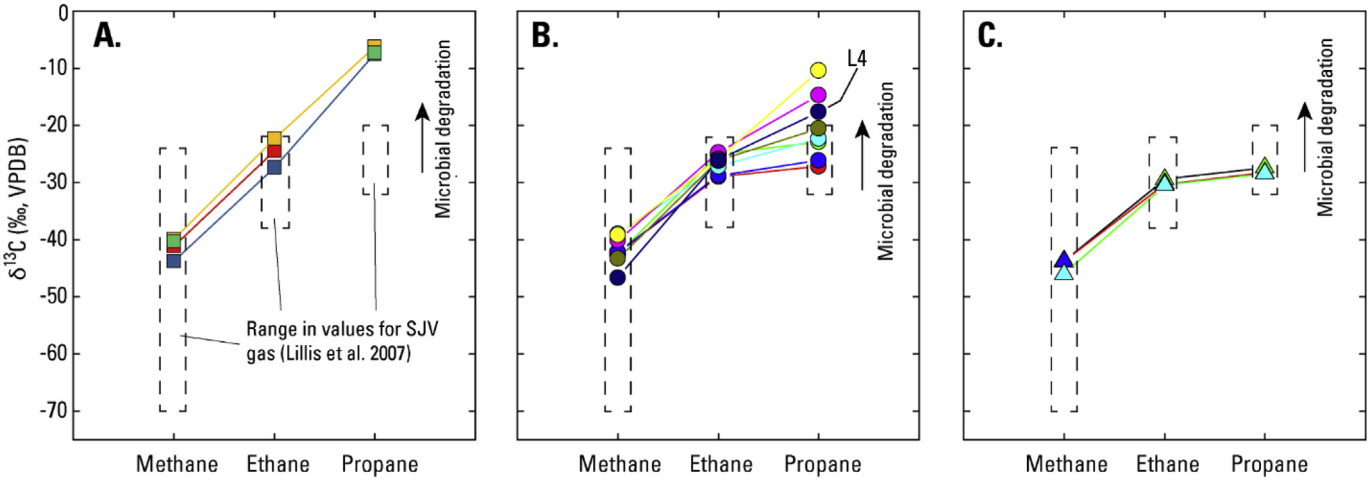

Fig. 8. $\delta^{13}C$ composition of methane, ethane, and propane in oil-field water from the (**A.**) Fruitvale, (**B.**) Lost Hills, and (**C.**) Belridge oil fields.

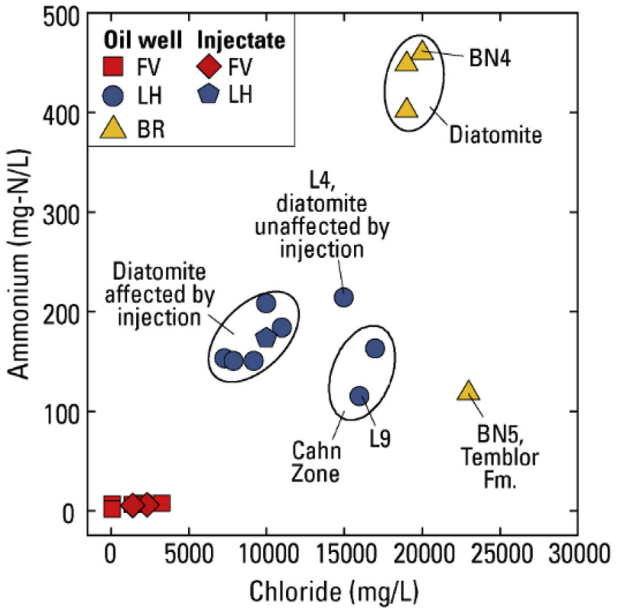

Fig. 9. Ammonium in relation to chloride concentrations in oil-field water. FV, Fruitvale; LH, Lost Hills; BR, Belridge.

2009). The data are generally consistent with that hypothesis. Sandstone is the primary lithology in the perforated intervals of sampled oil wells in Fruitvale, and the median $^{228}Ra/^{226}Ra$ ratio in samples from those wells is close to the global average $^{228}Ra/^{226}Ra$ ratio in sandstone (1.6) proposed by Vengosh et al. (2009) (Fig. 10C). $^{228}Ra/^{226}Ra$ ratios in the Lost Hills and Belridge samples are lower than the global average ratio for sandstone and more like the calculated $^{228}Ra/^{226}Ra$ activity ratios in sediments within the perforated intervals of the sampled oil wells in those fields (Fig. 10C). $^{228}Ra/^{226}Ra$ ratios in the sediments were calculated from Th/U concentration ratios in the sediments, as derived from spectral gamma-ray log output collected in several of the wells (California Department of Conservation, 2018c), using the approach of Kraemer and Reid (1984). Median $^{228}Ra/^{226}Ra$ ratios in the sampled diatomite- and Cahn-zone sediments (0.9 and 0.5, respectively) are within a factor of ~2 of the ratios in water from those zones.

$^{224}Ra/^{228}Ra$ ratios range from 0.2 to 9.5 (Fig. 10D). The median $^{224}Ra/^{228}Ra$ ratio in Fruitvale samples (1.5) was like the median ratio for samples from diatomite zones in the Lost Hills and Belridge fields (1.6). $^{224}Ra/^{228}Ra$ ratios above secular equilibrium ($^{224}Ra/^{228}Ra > 1$) are commonly observed in groundwater systems (Vengosh et al., 2009; Szabo et al., 2012; Vinson et al., 2013) and reflect the net effect of alpha-recoil release of the short-lived ^{224}Ra from solids and adsorption of Ra on solids surfaces (Hancock and Murray, 1996; Vengosh et al., 2009). The $^{224}Ra/^{228}Ra > 1$ that characterizes most of the SJV oil-field water suggests *in-situ* water-rock interactions (i.e., contemporary mobilization of Ra from the host rocks).

5. Conclusions

Chemical and isotopic data collected from oil wells, injection-water sources, and disposal ponds in four oil fields in the southern San Joaquin Valley were used to characterize regional patterns in the geochemistry of oil-field water. We show that the salinity and chemical composition of the oil-field water are due to the modification of an original seawater source by depth (temperature) and lithology dependent diagenetic processes and meteoric-water dilution. Meteoric water penetrates to depths of at least 1350 m on the east side of the valley due to relatively large natural sources of recharge, such as the Kern River, coming off the adjacent Sierra Nevada Mountains. Natural flushing of oil-bearing zones is less apparent on the west side of the valley, but the effects of water and steam injection for EOR, produced water disposal, and/or hydraulic fracturing on isotopic, inorganic, or radiochemical analytes in selected samples are evident. In addition to mixing with naturally recharged and injected fluids, other processes contributing to geochemical variability in oil-field water include preferential biodegradation of acetate and propane, and mobilization of ammonium and radium. The data illustrate the complexity of natural and human processes affecting the geochemistry of oil-field water in the southern San Joaquin Valley and underscore the importance of thoroughly characterizing potential oil-field water end members in groundwater-quality forensic studies.

Declarations of interest

None.

Acknowledgments

We thank well owners who allowed us to sample their wells. This article was improved by the constructive reviews of Peter Birkle, Mark Engle, Kimberly Taylor, and anonymous reviewers for the journal. This work was funded by the California State Water Resources Control Board's Regional Groundwater Monitoring in Areas of Oil and Gas Production Program and the USGS Cooperative Water Program. Any use of trade, firm, or product names is for description purposes only and does not imply endorsement by the U.S. Government.

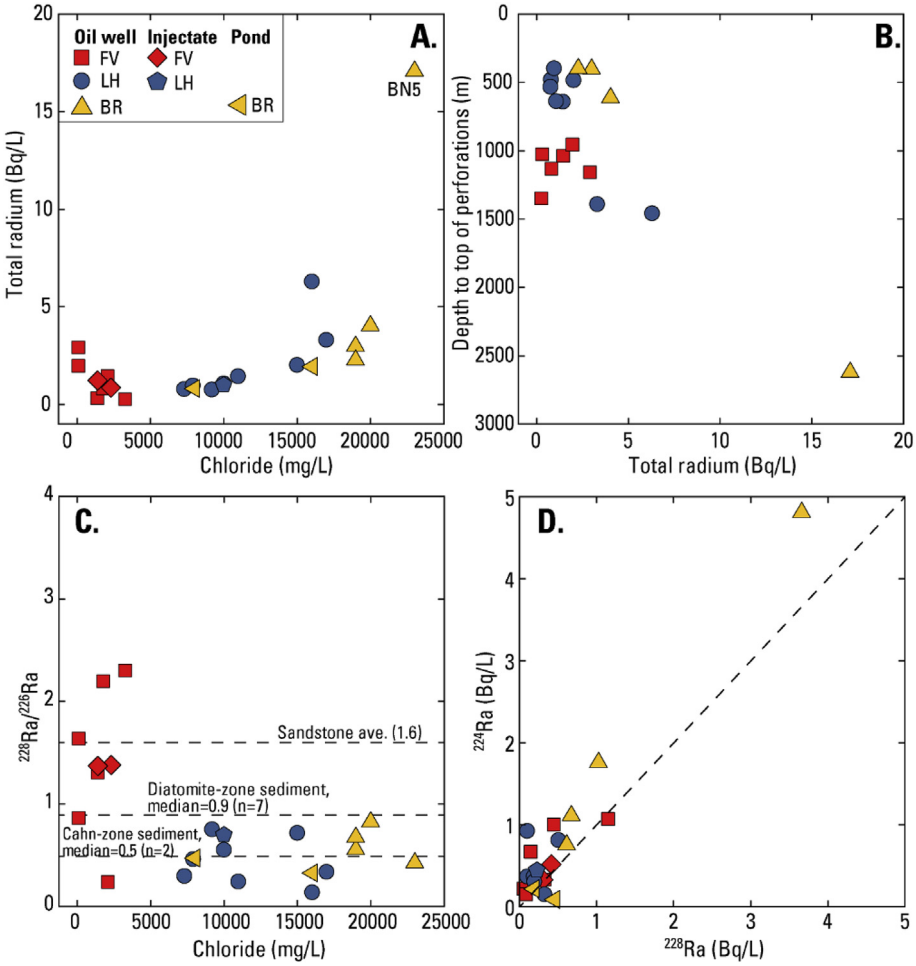

Fig. 10. (**A.**) Chloride concentrations and (**B.**) depth to the top of well perforations in relation to total radium activity in oil-field water; (**C.**) $^{228}Ra/^{226}Ra$ ratios in relation to chloride concentrations; and (**D.**) ^{224}Ra in relation to ^{228}Ra activities. FV, Fruitvale; LH, Lost Hills; BR, Belridge. In **C.**, sandstone average from Vengosh et al. (2009); median values for diatomite- and Cahn-zone sediments estimated from output from spectral gamma-ray logs (California Department of Conservation, 2018b).

Appendix A. Supplementary data

Supplementary data to this article can be found online at https://doi.org/10.1016/j.apgeochem.2018.09.015.

References

Baadsgaard, H., 1987. Rb-Sr and K-Ca isotope systematics in minerals from potassium horizons in the Prairie Evaporite formation, Saskatchewan, Canada. Chem. Geol. (Isot. Geosci. Sec.) 66, 1–15.

Ballentine, C.J., Sherwood Lollar, B., 2002. Regional groundwater focusing of nitrogen and noble gases into the Hugoton-Panhandle giant gas field, USA. Geochem. Cosmochim. Acta 66, 2483–2497.

Barry, P.H., Kulongoski, J.T., Landon, M.K., Tyne, R.L., Gillespie, J.M., Stephens, M.J., Hillegonds, D.J., Byrne, D.J., Ballentine, C.J., 2018. Tracing enhanced oil recovery signatures in casing gases from the Lost Hills oil field using noble gases. Earth Planet Sci. Lett. 496, 57–67.

Blondes, M.S., Gans, K.D., Engle, M.A., Kharaka, Y.F., Reidy, M.E., Saraswathula, V., Thordsen, J.J., Rowan, E.L., Morrissey, E.A., 2017. U.S. Geological Survey National Produced Waters Geochemical Database v2.3 (PROVISIONAL). https://energy.usgs.gov/EnvironmentalAspects/EnvironmentalAspectsofEnergyProductionandUse/ProducedWaters.aspx#3822349-data, Accessed date: 16 February 2018.

Boles, J.R., 1982. Active albitization of plagioclase, Gulf Coast tertiary. Am. J. Sci. 282, 165–180.

Boles, J.R., 1998. Carbonate cementation in tertiary sandstones, san Joaquin basin, California. Special Publ. Int. Assoc. Sedimentol. 26, 261–283.

Brueckner, H.K., Snyder, W.S., 1985. Chemical and Sr-isotopic variations during diagenesis of Miocene siliceous sediments of the Monterey Formation, California. J. Sediment. Petrol. 55, 553–568.

California Department of Conservation, 1996. A Study of NORM Associated with Oil and Gas Production Operations in California. 62 pp.

California Department of Conservation, 1998. California Oil & Gas Fields. Division of Oil, Gas, and Geothermal Resources, vol. 1 Central California. 507 pp.

California Department of Conservation, 2018a. Oil & Gas Online Data. Division of Oil, Gas, and Geothermal Resources. http://www.conservation.ca.gov/dog/Online_Data/Pages/Index.aspx, Accessed date: 20 February 2018.

California Department of Conservation, 2018b. Well stimulation treatment disclosures. ftp://ftp.consrv.ca.gov/pub/oil/Well_Stimulation_Treatment_Disclosures/Historical%20Disclosure%20Data/, Accessed date: 20 February 2018.

California Department of Conservation, 2018c. Division of oil, gas, and geothermal resources - well search. https://secure.conservation.ca.gov/WellSearch/, Accessed date: 20 February 2018.

California State Water Resources Control Board, 2018. Water Quality in Areas of Oil and Gas Production. https://www.waterboards.ca.gov/water_issues/programs/groundwater/sb4/, Accessed date: 25 April 2018.

Carothers, W.W., Kharaka, Y.K., 1978. Aliphatic acid anions in oil-field waters–Implications for origin of natural gas. Am. Assoc. Petrol. Geol. Bull. 62, 2441–2453.

Carothers, W.W., Kharaka, Y.K., 1980. Stable carbon isotopes of HCO_3^- in oil-field waters–implications for the origin of CO_2. Geochem. Cosmochim. Acta 44, 323–332.

Cathles, L.M., Schoell, M., Simon, R., 1987. CO2 generation during steamflooding: a geologically based kinetic theory that includes carbon isotope effects and application to high-temperature steamfloods. Soc. Petrol. Engin. 16267, 255–270.

Central Valley Regional Water Quality Control Board, 2018. Oil Fields Information – Disposal Ponds. https://www.waterboards.ca.gov/centralvalley/water_issues/oil_fields/information/disposal_ponds/, Accessed date: 23 April 2018.

Coburn, M.G., Gillespie, J.M., 2002. A hydrologic study to optimize steamflood performance in a giant oil field: Kern River field, California. Am. Assoc. Petrol. Geol. Bull. 86, 1489–1505.

Compton, J.S., Williams, L.B., Ferrel, R.E., 1992. Mineralization of organogenic ammonium in the Monterey Formation, Santa maria and san Joaquin basins, California, USA. Geochem. Cosmochim. Acta 56, 1979–1991.

Coplen, T.B., Kendall, C., 2000. Stable Hydrogen and Oxygen Isotope Ratios for Selected Sites of the U.S. Geological Survey's Nasqan and Benchmark Surface-Water Network.

U.S. Geol. Surv. Open-File Repp. 00–160.
Craig, H., 1966. Isotopic composition and origin of the red sea and salton sea geothermal brines. Science 154, 1544–1548.
Darrah, T.H., Vengosh, A., Jackson, R.A., Warner, N.R., Poreda, R.J., 2014. Noble gases identify the mechanisms of fugitive gas contamination in drinking-water wells overlying the Marcellus and Barnett Shales. Proc. Natl. Acad. Sci. U.S.A. 111, 14076–14081.
Davis, G.H., Coplen, T.B., 1989. Late cenozoic paleohydrogeology of the western san Joaquin Valley, California, as related to structural movements in the central Coast ranges. Geol. Soc. Am. Spec. Pap. 234.
Davis, T.A., Kulongoski, J.T., McMahon, P.B., 2016. Produced Water Chemistry Data for Samples from Four Petroleum Wells, Southern San Joaquin Valley, California, 2014. U.S. Geol. Surv. Data Release. https://doi.org/10.5066/F7XG9P83, Accessed date: 13 August 2018.
Davis, T.A., 2018. Water chemistry data for samples collected at groundwater and surface-water sites near the Lost Hills and Belridge oil fields, November 2016–September 2017, Kern County, California. U.S. Geol. Surv Data Release. https://doi.org/10.5066/F7NS0T5M, Accessed date: 13 September 2018.
DePaolo, D.J., Finger, K.L., 1991. High-resolution strontium-isotope stratigraphy and biostratigraphy of the Miocene Monterey Formation, central California. Geol. Soc. Am. Bull. 103, 112–124.
Engle, M.A., Reyes, F.R., Varonka, M.S., Orem, W.H., Ma, L., Ianno, A.J., Schell, T.M., Xu, P., Carroll, K.C., 2016. Geochemistry of formation waters from the Wolfcamp and "Cline" shales: insights into brine origin, reservoir connectivity, and fluid flow in the Permian Basin, USA. Chem. Geol. 425, 76–92.
Fisher, J.B., Boles, J.R., 1990. Water-rock interaction in Tertiary sandstones, San Joaquin basin, California, U.S.A: Diagentic controls on water composition. Chem. Geol. 82, 83–101.
Gannon, R., Saraceno, J.F., Kulongoski, J.T., Teunis, J.A., Barry, P.H., Tyne, R.L., Kraus, T.E.C., Hansen, A.M., Qi, S.L., 2018. Produced water chemistry data for the Lost Hills, Fruitvale, and North and South Belridge study areas, Southern San Joaquin Valley, California. U.S. Geol. Surv Data Release. https://doi.org/10.5066/F7X929H9, Accessed date: 13 August 2018.
Gans, K.D., Metzger, L.F., Gillespie, J.M., Qi, S.L., 2018. Historical produced water chemistry data compiled for the Fruitvale Oilfield, Kern County, California. U.S. Geol. Surv Data Release. https://doi.org/10.5066/F72B8X8G, Accessed date: 13 August 2018.
Hancock, G.J., Murray, A.S., 1996. Source and distribution of dissolved radium in the Bega River estuary, southeastern Australia. Earth Planet Sci. Lett. 138, 145–155.
Harkness, J.S., Dwyer, G.S., Warner, N.R., Parker, K.M., Mitch, W.A., Vengosh, A., 2015. Iodide, bromide, and ammonium in hydraulic fracturing and oil and gas wastewaters: Environmental implications. Environ. Sci. Technol. 49, 1955–1963.
Harkness, J.S., Darrah, T.H., Warner, N.R., Whyte, C.J., Moore, M.T., Millot, R., Kloppmann, W., Jackson, R.B., Vengosh, A., 2017. The geochemistry of naturally occurring methane and saline groundwater in an area of unconventional shale gas development. Geochem. Cosmochim. Acta 208, 302–334.
Harkness, J.S., Warner, N.R., Ulrich, A., Millot, R., Kloppmann, W., Ahad, J.M.E., Savard, M.M., Gammon, P., Vengosh, A., 2018. Characterization of the boron, lithium, and strontium isotopic variations of oil sands process-affected water in Alberta, Canada. Appl. Geochem. 90, 50–62.
Hayes, M.J., Boles, J.R., 1993. Evidence for meteoric recharge in the San Joaquin basin, California provided by isotope and trace element chemistry of calcite. Mar. Petrol. Geol. 10, 135–144.
Hluza, A.G., 1965. Summary of Operations, California Oil Fields, vol. 51 California Department of Conservation, Division of Oil and Gas.
Humez, P., Mayer, B., Ing, J., Nightingale, M., Becker, V., Kingston, A., Akbilgic, O., Taylor, S., 2016. Occurrence and origin of methane in groundwater in Alberta (Canada): Gas geochemical and isotopic approaches. Sci. Total Environ. 541, 1253–1268.
James, A.T., Burns, B.J., 1984. Microbial alteration of subsurface natural gas accumulations. Am. Assoc. Petrol. Geol. Bull. 68, 957–960.
Jones, D.M., Head, I.M., Gray, N.D., Adams, J.J., Rowan, A.K., Aitken, C.M., Bennett, B., Huang, H., Brown, A., Bowler, B.F.J., Oldenburg, T., Erdmann, M., Larter, S.R., 2008. Crude-oil biodegradation via methanogenesis in subsurface petroleum reservoirs. Nature 451, 176–180.
Jordan, P., Heberger, M., 2014. Historical and current application of well stimulation technology in California. In: Advanced Well Stimulation Technologies in California, Executive Summary. California Council on Science and Technology, pp. 89–120.
Keith, M.L., Weber, J.N., 1964. Carbon and oxygen isotopic composition of selected limestones and fossils. Geochem. Cosmochim. Acta 28, 1787–1816.
Kharaka, Y.K., Berry, F.A.F., 1973. Isotopic composition of oil-field brines from Kettleman North Dome, California, and their geologic implications. Geochem. Cosmochim. Acta 37, 1899–1908.
Kharaka, Y.K., Otton, J.K., 2007. Preface to special issue on environmental issues related to oil and gas production. Appl. Geochem. 22, 2095–2098.
Kharaka, Y.K., Hanor, J.S., 2014. Deep fluids in sedimentary basins. In: Holland, H., Turekian, K. (Eds.), Treatise on Geochemistry, second ed. Elsevier Science, Amsterdam, pp. 471–515.
Kraemer, T.F., Reid, D.F., 1984. The occurrence and behavior of radium in saline formation water of the U.S. Gulf Coast region. Isot. Geosci. 2, 153–174.
Kulongoski, J.T., McMahon, P.B., Land, M.T., Wright, M.T., Johnson, T.A., Landon, M.K., 2018. Origin of methane and sources of high concentrations in Los Angeles groundwater. J. Geophys. Res.: Biogeosciences 123. https://doi.org/10.1002/2017JG004026.
Land, P.E., 1984. Lost Hills Oil Field. California Department of Conservation, Division of Oil and Gas TR32.
Land, L.S., Macpherson, G.L., 1992. Origin of saline formation waters, Cenozoic section, Gulf of Mexico sedimentary basin. Am. Assoc. Petrol. Geol. Bull. 76, 1344–1362.
Lauer, N.E., Harkness, J.S., Vengosh, A., 2016. Brine spills associated with unconventional oil development in North Dakota. Environ. Sci. Technol. 50, 5389–5397.
Lico, M.S., Kharaka, Y.K., Carothers, W.W., Wright, V.A., 1982. Methods for Collection and Analysis of Geopressured Geothermal and Oil Field Waters. U.S. Geol. Surv. Water-Supply Paper 2194.
Lillis, P.G., Warden, A., Claypool, G.E., Magoon, L.B., 2007. Petroleum systems of the San Joaquin basin province–Geochemical characteristics of gas types. In: Scheirer, A.H. (Ed.), Petroleum Systems and Geologic Assessment of Oil and Gas in the San Joaquin Basin Province, California. U.S. Geol. Surv. Prof, Paper 1713, Ch. 10.
McIntosh, J.C., Warwick, P.D., Martini, A.M., Osborn, S.G., 2010. Coupled hydrology and biogeochemistry of Paleocene-Eocene coal beds, northern Gulf of Mexico. Geol. Soc. Am. Bull. 122, 1248–1264.
McMahon, P.B., Barlow, J.R.B., Engle, M.A., Belitz, K., Ging, P.B., Hunt, A.G., Jurgens, B.C., Kharaka, Y.K., Tollett, R.W., Kresse, T.M., 2017. Methane and benzene in drinking-water wells overlying the Eagle Ford, Fayetteville, and Haynesville Shale hydrocarbon production areas. Environ. Sci. Technol. 51, 6727–6734.
Milkov, A.V., 2011. Worldwide distribution and significance of secondary microbial methane formed during petroleum biodegradation in conventional reservoirs. Org. Geochem. 42, 184–207.
Murata, K.J., Friedman, I., Madsen, B.M., 1969. Isotopic Composition of Diagenetic Carbonates in Marine Miocene Formations of California and Oregon. U.S. Geol. Surv. Prof. Paper 614–B.
Nicot, J.-P., Larson, T., Darvari, R., Mickler, P., Slotten, M., Aldridge, J., Uhlman, K., Costely, R., 2017. Controls on Methane Occurrence in Shallow Aquifers Overlying the Haynesville Shale Gas Field, East Texas. Groundwater. https://doi.org/10.1111/gwat.12500.
Orem, W.H., Tatu, C., Varonka, M., Lerch, H., Bates, A., Engle, M., Crosby, L., McIntosh, J., 2014. Organic substances in produced and formation water from unconventional natural gas extraction in coal and shale. Int. J. Coal Geol. 126, 20–31.
Preston, H.M., 1931. Summary of Operations, California Oil Fields, vol. 16 California Department of Natural Resources, Division of Oil and Gas.
Rowan, E.L., Engle, M.A., Kraemer, T.F., Kirby, C., 2011. Radium content of oil and gas field produced waters in the northern Appalachian basin (USA): Summary of data. U.S. Geol. Surv. Sci. Invest. Rep. 2011–5135.
Rozanski, K., Araguás- Araguás, L., Gonfiantini, R., 1993. Isotopic patterns in modern global precipitation. In: Swart, P.K., Lohmann, K.C., McKenzie, J., Savin, S. (Eds.), Climate Change in Continental Isotopic Records. vol. 78. American Geophysical Union, Geophysical Monograph, pp. 1–36.
Scheirer, A.H., Magoon, L.B., 2007. Age, distribution, and stratigraphic relationship of rock units in the San Joaquin Basin Province, California. In: Scheirer, A.H. (Ed.), Petroleum Systems and Geologic Assessment of Oil and Gas in the San Joaquin Basin Province, California. U.S. Geol. Surv. Prof, Paper 1713, Ch. 5.
Schlegel, M.E., McIntosh, J.C., Petsch, S.T., Orem, W.H., Jones, E.J.P., Martini, A.M., 2013. Extent and limits of biodegradation by in situ methanogenic consortia in shale and formation fluids. Appl. Geochem. 28, 172–184.
Schloemer, S., Elbracht, J., Blumenberg, M., Illing, C.J., 2016. Distribution and origin of dissolved methane, ethane and propane in shallow groundwater of Lower Saxony, Germany. Appl. Geochem. 67, 118–132.
Schoell, M., 1980. The hydrogen and carbon isotopic composition of methane from natural gases of various origins. Geochem. Cosmochim. Acta 44, 649–661.
Schwartz, D.E., 1988. Characterizing the lithology, petrophysical properties, and depositional setting of the Belridge diatomite, South Belridge field, Kern County, California. In: Graham, S.A. (Ed.), Studies of the Geology of the San Joaquin Basin. Pacific Section SEPM 60, pp. 281–301.
Schultz, J.L., Boles, J.R., Tilton, G.R., 1989. Tracking calcium in the San Joaquin basin, California: A strontium isotopic study of carbonate cements at North Coles Levee. Geochem. Cosmochim. Acta 53, 1991–1999.
Shelton, J.L., Pimentel, I., Fram, M.S., Belitz, K., 2008. Ground-Water Quality Data in the Kern County Subbasin Study Unit, 2006—Results from the California GAMA Program. U.S. Geol. Surv. Data Series 337.
Szabo, Z., DePaul, V.T., Fischer, J.M., Kraemer, T.F., Jacobsen, E., 2012. Occurrence and geochemistry of radium in water from principal drinking-water aquifer systems of the United States. Appl. Geochem. 27, 729–752.
Taylor, T.R., Soule, C.H., 1993. Reservoir characterization and diagenesis of the Oligocene 64-Zone Sandstone, North Belridge field, Kern County, California. Am. Assoc. Petrol. Geol. Bull. 77, 1549–1566.
Thurman, E.M., 1985. Organic Geochemistry of Natural Waters. Martinus Nijhoff/Dr W. Junk, Boston.
Tyne, R.L., Barry, P.H., Kulongoski, J.T., Landon, M.K., Hillegonds, D.J., McMahon, P.B., Ballentine, C.J., 2018. Noble gas characterization of produced waters from the Fruitvale and Lost Hills oil fields, CA, USA. In: Goldschmidt Conference, Aug. 12–17, Boston, MA, . https://goldschmidt.info/, Accessed date: 14 August 2018.
Veizer, J., 1989. Strontium isotopes in seawater through time. Annu. Rev. Earth Planet Sci. 17, 141–167.
Vengosh, A., Hirschfeld, D., Vinson, D., Dwyer, G., Raanan, H., Rimawi, O., Al-Zoubi, A., Akkawi, E., Marie, A., Haquin, G., Zaarur, S., Ganor, J., 2009. High naturally occurring radioactivity in fossil groundwater from the Middle East. Environ. Sci. Technol. 43, 1769–1775.
Vinson, D.S., Tagma, T., Bouchaou, L., Dwyer, G.S., Warner, N.R., Vengosh, A., 2013. Occurrence and mobilization of radium in fresh to saline coastal groundwater inferred from geochemical and isotopic tracers. Appl. Geochem. 38, 161–175.
Warner, N.R., Darrah, T.H., Jackson, R.B., Millot, R., Kloppmann, W., Vengosh, A., 2014. New tracers identify hydraulic fracturing fluids and accidental releases from oil and gas operations. Environ. Sci. Technol. 48, 12552–12560.

Weis, D., Wasserburg, G.J., 1987. Rb-Sr and Sm-Nd systematics of cherts and other siliceous deposits. Geochem. Cosmochim. Acta 51, 959–972.
Wen, T., Castro, M.C., Nicot, J.P., Hall, C.M., Larson, T., Mickler, P., Darvari, R., 2016. Methane sources and migration mechanisms in shallow groundwaters in Parker and Hood Counties, Texas–A heavy noble gas analysis. Environ. Sci. Technol. 50, 12012–12021.
Whiticar, M.J., Faber, E., Schoell, M., 1986. Biogenic methane formation in marine and freshwater environments: CO2 reduction vs. acetate fermentation–Isotope evidence. Geochem. Cosmochim. Acta 50, 693–709.
Williams, L.B., Ferrel, R.E., Hutcheon, I., Bakel, A., Walsh, M.M., Krouse, H.R., 1995. Nitrogen isotope geochemistry of organic matter and minerals during diagenesis and hydrocarbon migration. Geochem. Cosmochim. Acta 59, 765–779.
Williams, A.E., Rodoni, D.P., 1997. Regional isotope effects and application to hydrologic investigations in southwestern California. Water Resour. Res. 33, 1721–1729.
Zheng, Z., Zhang, H., Chen, Z., Li, X., Zhu, P., Cui, X., 2017. Hydrogeochemical and isotopic indicators of hydraulic fracturing flowback fluids in shallow groundwater and stream water, derived from Dameigou Shale gas extraction in the northern Qaidam Basin. Environ. Sci. Technol. 51, 5889–5898.